IAI Journals.ASM.org

Characterization of Immunological Cross-Reactivity between Enterotoxigenic *Escherichia coli* Heat-Stable Toxin and Human Guanylin and Uroguanylin

Arne M. Taxt,[a,b] Yuleima Diaz,[b] Amélie Bacle,[c] Cédric Grauffel,[c] Nathalie Reuter,[b,c] Rein Aasland,[b] Halvor Sommerfelt,[a,d] Pål Puntervoll[b,e]

Centre for International Health, Department of Global Public Health and Primary Care, University of Bergen, Bergen, Norway[a]; Department of Molecular Biology, University of Bergen, Bergen, Norway[b]; Computational Biology Unit, Uni Research AS, Bergen, Norway[c]; Division of Infectious Disease Control, Norwegian Institute of Public Health, Oslo, Norway[d]; Centre for Applied Biotechnology, Uni Environment, Uni Research AS, Bergen, Norway[e]

Enterotoxigenic *Escherichia coli* (ETEC) expressing the heat-stable toxin (ST) (human-type [STh] and porcine-type [STp] variants) is among the five most important enteric pathogens in young children living in low- and middle-income countries. ST mediates diarrheal disease through activation of the guanylate cyclase C (GC-C) receptor and is an attractive vaccine target with the potential to confer protection against a wide range of ETEC strains. However, immunological cross-reactivity to the endogenous GC-C ligands guanylin and uroguanylin is a major concern because of the similarities to ST in amino acid sequence, structure, and function. We have investigated the presence of similar epitopes on STh, STp, guanylin, and uroguanylin by analyzing these peptides in eight distinct competitive enzyme-linked immunosorbent assays (ELISAs). A fraction (27%) of a polyclonal anti-STh antibody and an anti-STh monoclonal antibody (MAb) cross-reacted with uroguanylin, the latter with a 73-fold-lower affinity. In contrast, none of the antibodies raised against STp, one polyclonal antibody and three MAbs, cross-reacted with the endogenous peptides. Antibodies raised against guanylin and uroguanylin showed partial cross-reactivity with the ST peptides. Our results demonstrate, for the first time, that immunological cross-reactions between ST and the endogenous peptides can occur. However, the partial nature and low affinity of the observed cross-reactions suggest that the risk of adverse effects from a future ST vaccine may be low. Furthermore, our results suggest that this risk may be reduced or eliminated by basing an ST immunogen on STp or a selectively mutated variant of STh.

The heat-stable toxin (ST) of enterotoxigenic *Escherichia coli* (ETEC) has recently been given renewed attention as a vaccine target (1–7). A large multicenter study on the etiology of diarrheal disease in children <5 years of age found ST-expressing ETEC (with or without the heat-labile toxin) to be among the five most important causes of moderate-to-severe diarrhea (8) in low- and middle-income countries. ST is present in approximately 75% of ETEC strains (9), and two variants of the toxin have been identified, namely, the human type (STh) and the porcine type (STp). These are highly conserved, and no clinically relevant sequence variants have been reported. STh-expressing ETEC strains appear to be more closely associated with diarrhea than strains that express STp (10), which suggests that vaccine development should target primarily the former. The STs are small (~2,000-Da) haptens capable of engendering immune responses in animals when coupled to a carrier molecule (11–13). ST, also referred to as STa, is structurally, functionally, and immunologically distinct from the larger ETEC STb, which can cause disease in animals but not in humans (14).

ST activates the guanylate cyclase C (GC-C) receptor, which is present on the luminal surface of intestinal epithelial cells, thereby triggering a strong efflux of salt and water into the intestinal lumen, which presents clinically as diarrhea (15, 16). The endogenous GC-C ligands guanylin and uroguanylin also activate the GC-C receptor and are involved in the regulation of water and electrolyte transport. ST has been reported to be 10-fold more potent than uroguanylin and 100-fold more potent than guanylin in activating the GC-C receptor (17). An X-ray structure of the toxic domain of a synthetic analog of STp, consisting of amino acid residues Cys5 to Cys17, and where Cys5 was replaced by β-mercaptopropionic acid, shows that ST forms a right-handed spiral, which is stabilized by three disulfide bridges in a 1-4/2-5/3-6 pattern (18). Nuclear magnetic resonance (NMR) analyses have shown that guanylin and uroguanylin can adopt two distinct topological forms, forms A and B, of which only form A is biologically active and similar to the ST structure (19, 20). In contrast to ST, the endogenous ligands have only two disulfide bridges in a 1-3/2-4 pattern, which are analogous to the ST 2-5/3-6 bridges. It has been suggested that the ST-specific disulfide bridge locks ST in a conformation that resembles the active A form of the endogenous ligands (21). Both ST and the endogenous ligands have N-terminal tails, but structural information is available only for the endogenous ligands and suggests that the N termini are unstructured (19, 20). The structural similarity of the region from the first to the last shared cysteines of ST and the A forms of the endogenous ligands (the GC-C ligand domain) is reflected by low root mean square deviation (RMSD) values of 1.4 Å for guanylin/uroguanylin, 1.4 Å for STp/guanylin, and 1.1 Å for STp/uroguanylin (19, 20). In contrast, there is little structural similarity be-

Received 1 April 2014 **Accepted** 19 April 2014
Published ahead of print 28 April 2014
Editor: S. R. Blanke
Address correspondence to Pål Puntervoll, pal.puntervoll@uni.no.

doi:10.1128/IAI.01749-14

tween ST and the inactive B forms, as revealed by high RMSD values of 4.7 Å for STp/guanylin and 4.5 Å for STp/uroguanylin. On the sequence level, the peptides display moderate to high sequence identities in the GC-C ligand domain: 92% for STp/STh, 67% for guanylin/uroguanylin, 58% for STp/guanylin, 75% for STp/uroguanylin, 67% for STh/guanylin, and 83% for STh/uroguanylin. The compelling similarities in both sequence and structure have raised major concerns for ST vaccine development, namely, that antibodies against ST may cross-react with the endogenous GC-C ligands (1, 2, 9).

Guanylin and uroguanylin seem to carry out their functions mainly on the luminal side of the intestine (16, 22, 23), but uroguanylin can also be isolated from human urine (16, 24). In the bloodstream, the larger and inactive proforms of both guanylin and uroguanylin are present at much higher concentrations than those of the bioactive peptides (24). Several studies support the view postulated by Forte (16) that uroguanylin participates in an endocrine axis connecting the gastrointestinal tract with the kidneys in the regulation of body sodium balance (23, 25, 26). In addition, the GC-C receptor is expressed in the epididymis (27) and brain (28). Since guanylin, uroguanylin, and their cognate receptor GC-C are present in several body compartments, potential autoimmune reactions that interfere with GC-C-mediated signaling may have serious consequences.

Bacterial and viral infections may trigger autoimmune disease, and careful attention is given when antigens with known cross-reactive potential are evaluated for inclusion in vaccines. Autoimmune adverse effects of vaccination have been identified for both influenza and measles-mumps-rubella (MMR) vaccines. The 1976-1977 vaccination campaign against influenza (with the A/New Jersey/8/76 swine flu vaccine) resulted in an increased risk of Guillain-Barré syndrome (29, 30), and the currently used MMR vaccine has been reported to increase the risk of acquiring idiopathic-thrombocytopenic purpura (31, 32). Molecular mimicry that causes cross-reactivity and potential autoimmune reactions is also a well-known challenge to the development of vaccines against group A streptococci (33, 34), and the U.S. Food and Drug Administration (FDA) now requires extensive *in vitro* and animal data showing an absence of cross-reactivity before sanctioning human trials (35).

Since ST is nonimmunogenic, the autoimmune potential of this peptide will not be revealed before it is made immunogenic, e.g., by coupling to a carrier, and administered as a vaccine. It is, however, both possible and important to address the question of cross-reactivity at an early stage in vaccine development by assessing whether there is any similar epitope(s) between ST and the endogenous peptides. We are not aware of any such investigations, with the exception of a study where one antiguanylin monoclonal antibody (MAb) was tested against ST and showed no cross-reactivity (36). Hence, the aim of the present study was to investigate the presence of similar epitopes between STh, STp, guanylin, and uroguanylin. We have done so by the use of eight different competitive enzyme-linked immunosorbent assays (ELISAs). Four ELISAs were based on polyclonal antibodies to STh, STp, guanylin, and uroguanylin, respectively. In addition, we utilized four ELISAs based on anti-ST MAbs, one of which was described previously as being capable of neutralizing STh (ST:G8) (37) and three of which are commercially available anti-STp MAbs.

MATERIALS AND METHODS

Structural modeling and molecular dynamics simulations. Structural models of the full-length peptides of STh and STp were built by using MODELLER (38). The available experimental structures of the toxic domain of STp (PDB accession no. 1ETN) and the endogenous peptides guanylin (PDB accession no. 1GNA) and uroguanylin (PDB accession no. 1UYA) were used as templates. The structural model of STh and the solution structures of guanylin and uroguanylin were subjected to energy minimization by using Charmm (39), and subsequent molecular dynamics (MD) simulations were performed with the program NAMD2.9 (40, 41), using the Charmm27 force field (42, 43). The peptides were solvated in a cubic box (60 by 60 by 60 $Å^3$) of TIP3P water molecules by using Charmm GUI (44), which was also used to add sodium and chloride ions (0.15 M NaCl). The simulations were performed in the NPT ensemble at a temperature of 300 K and a pressure of 10^5 Pa, with an integration time step of 1 fs. A cutoff of 14 Å was used for the truncation of nonbonded integration. A switch function was used for van der Waals forces, and a shift function was used for electrostatics. The simulations consisted of four successive heating phases (10 K, 100 K, 200 K, and 300 K), a 100-ps-long equilibration phase, and a production phase of 20 ns.

Peptides. STh and STp peptides used in this study either were purified from ETEC and kindly provided by John D. Clements, Tulane University, and Donald C. Robertson, Kansas State University, or had been produced by chemical synthesis (Bachem AG, Bubendorf, Switzerland). Synthetic STp (catalog no. H-6248) was synthesized with specific disulfide bridges (i.e., Cys5-Cys10, Cys6-Cys14, and Cys9-Cys17), while STh was a custom-made synthesized air-oxidized peptide. The guanylin (catalog no. H-2996) and uroguanylin (catalog no. H-2166) synthetic peptides with native disulfide bridges (Cys4-Cys12 and Cys7-Cys15 for both peptides) were also prepared by Bachem. The biological activity of all peptides was confirmed by a T-84 cell assay, and the observed 50% effective concentrations (EC_{50}s) were 58 ± 9 nM for ETEC STh, 44 ± 6 nM for ETEC STp, 79 ± 10 nM for synthetic STh, 161 ± 26 nM for synthetic STp, 692 ± 101 nM for guanylin, and 174 ± 21 nM for uroguanylin.

Antibodies. Polyclonal anti-STh and anti-STp antibodies, kindly provided by John D. Clements, Tulane University, were raised against bovine serum albumin (BSA) conjugates in rabbits and protein A purified. The conjugates were prepared by glutaraldehyde conjugation of STh and STp, respectively. Anti-STh MAb ST:G8, kindly provided by Sandhya S. Visweswariah, Indian Institute of Science, was described previously (37). This MAb was raised against a mutant variant of STh (SThY19F) conjugated to BSA by using glutaraldehyde. Three anti-STp MAbs (Fitzgerald Industries International), clone 29 (catalog no. 10-1013), clone 30 (catalog no. 10-1014), and clone 31 (catalog no. 10-1015), were all raised against a conjugate where synthetic STp with native disulfide bridges (catalog no. H-6248; Bachem) was conjugated to keyhole limpet hemocyanin (KLH). The conjugation was performed to selectively target carboxyl groups, thus coupling STp to KLH via the C-terminal carboxyl group or Glu7. Polyclonal antiguanylin (catalog no. ab14344; Abcam, Cambridge, United Kingdom) was produced in rabbit and raised against a synthetic peptide with the sequence PGTCEICAYAACTGC. According to the manufacturer, the peptide was conjugated to KLH by using 1-ethyl-3-(3-dimethylaminopropyl)carbodiimide hydrochloride (EDC). The antiuroguanylin antibody (catalog no. sc-32578, lot no. J2010; Santa Cruz Biotechnology, Dallas, TX) was an affinity-purified polyclonal antibody produced in goat. The antibody was raised against a peptide that maps to the C terminus of human uroguanylin. Polyclonal antibodies used as negative controls were anti-GST rabbit polyclonal antibody (raised against glutathione *S*-transferase [GST]) (catalog no. sc-459; Santa Cruz Biotechnology) and anti-NATH rabbit polyclonal antibody (custom antibody raised against *N*-acetyltransferase, human; Biogenes GmbH, Berlin, Germany). The following secondary antibodies where purchased from Sigma-Aldrich (St. Louis, MO): anti-rabbit (IgG alkaline phosphatase conjugate A8025) for use in the STh ELISA, STp ELISA, and guanylin ELISA; anti-goat (IgG alkaline phosphatase conjugate A4187) for the uroguany-

lin ELISA; and anti-mouse (IgG alkaline phosphatase conjugate A4312) for all MAb ELISAs.

Conjugation procedure for ELISA coating. The conjugates used for ELISA coating in the STp ELISA, the STh ELISA, and the MAb ELISAs for ST:G8, clone 29, and clone 30 were prepared by glutaraldehyde conjugation of ST to ovalbumin according to a protocol modified from the one described previously by Lockwood and Robertson (11). The sources of ST were ETEC STp for the STp ELISA, ETEC STh for the STh ELISA, and synthetic STh for the MAb ELISAs. Briefly, 200 μg ST was conjugated to 450 μg ovalbumin (Sigma-Aldrich) by adding 600 μg glutaraldehyde (Sigma-Aldrich) in 0.1 M phosphate buffer (pH 6.8), in a total reaction mixture volume of 1 ml. The reaction was allowed to proceed for 2 h with gentle stirring in the dark at room temperature. The reaction was stopped by the addition of 10 μl 1 M L-lysine (Sigma-Aldrich), and the mixture was stirred gently for another 30 min. The conjugate was then dialyzed against phosphate-buffered saline (PBS) for 24 h at 4°C by using Spectrapor dialysis tubing (molecular mass cutoff of 10 kDa) and stored at −20°C until use.

Mass spectrometry. Mass analysis was performed by using an Ultraflex MALDI ToF/ToF mass spectrometer (Bruker Daltonics, Billerica, MA). Samples were desalted and prepared for analysis as described previously (45), using a matrix solution consisting of 8 g/liter alfa-cyano-4-hydroxycinnamic acid (CHCA), 60% acetonitrile, 15% methanol, and 0.1% trifluoroacetic acid (TFA). We also analyzed peptides after treatment with dithiothreitol (DTT) and iodoacetamide for reduction and alkylation of cysteines, as described previously (46). The mass spectrometer was calibrated prior to use with Peptide Calibration Standard II (Bruker Daltonics).

T-84 cell assay. T-84 cells (ATCC) were seeded and grown to confluence on 24-well plates (Nunc, Roskilde, Denmark) in Dulbecco's modified Eagle medium (DMEM)–F-12 medium (Lonza, Walkersville, MD) supplemented with 10% fetal bovine serum and 0.2% gentamicin. Cells were washed 3 times with 500 μl DMEM–F-12 medium and preincubated with 200 μl DMEM containing 1 mM 3-isobutyl-1-methylxanthine for 45 to 60 min at 37°C. Serial dilutions of peptides to be tested were diluted in 200 μl DMEM–F-12 medium, added to each well, and incubated for 60 min at 37°C. Samples were tested in duplicate wells. Following incubation, the reaction medium was aspirated, and the cells were lysed with 0.1 M HCl at 20°C for 20 min. In some instances, the cells were also freeze-thawed three times to ensure complete lysis. The lysates were centrifuged at 16,000 × *g* for 10 min, and supernatants were collected for analysis. Cyclic GMP (cGMP) levels were measured by using a commercial cGMP enzyme immunoassay kit (Enzo Life Sciences Inc.) according to the manufacturer's instructions.

T-84 cell assay neutralization experiments. For neutralization experiments, 10 ng STh was preincubated overnight at 4°C with polyclonal antibody diluted in 200 μl DMEM–F-12 medium. Antibody dilutions of 1:10, 1:50, and 1:100 were tested. For neutralization experiments with MAbs, the protocol was slightly modified: MAbs were diluted in PBS containing 0.2% bovine serum albumin and were preincubated with 10 ng ST for 1 h at room temperature prior to addition to T-84 cells. Neutralization experiments with MAbs were carried out with STh and STp. The T-84 cell assay was performed as described above to test the biological activity of the preincubated sample.

Competitive ST ELISAs. Competitive ST ELISAs using polyclonal anti-STh and anti-STp antibodies were performed as described previously (4, 11, 47), with minor modifications. Briefly, microtiter plates were coated with STh or STp ovalbumin conjugates (0.11 μg per well for STh and 0.16 μg per well for STp) in 150 μl ELISA buffer (128 mM NaCl, 2.7 mM KCl, 1.5 mM KH_2PO_4, 8.1 mM Na_2HPO_4 [pH 7.2]) overnight at 37°C. Wells were then washed and blocked with 1% ovalbumin in ELISA buffer for 1 h at 37°C. Seventy-five microliters of sample was mixed with 75 μl of diluted primary antibody (anti-STh, 1:2,000 final dilution; anti-STp, 1:10,000 final dilution) and incubated for 2 h at 37°C. After washing, the plate was incubated with 100 μl anti-rabbit secondary antibody (dilution, 1:400) for 1 h at room temperature. The plate was then developed for approximately 30 min by using 100 μl freshly prepared developing buffer (1 mg/ml *para*-nitrophenylphosphate (pNPP) in 9.7% [vol/vol] 0.5 mM $MgCl_2 \cdot 6H_2O$ [pH 9.8]), development was stopped by the addition of 50 μl 2 M NaOH, and the optical density at 405 nm (OD_{405}) was measured.

The competitive ELISAs using the ST:G8, clone 29, and clone 30 monoclonal antibodies were similar and differed only in coating and antibody concentrations. Briefly, ELISA plates (Nunc Immobilizer Amino) were coated with 100 μl of the STh-ovalbumin conjugate in PBS (146 mM NaCl, 4 mM Na_2HPO_4, 1.1 mM KH_2PO_4 [pH 7.2]) and incubated overnight at 4°C. For the ST:G8 ELISA, 0.020 μg conjugate per well was used; for clone 29 and clone 30, plates were coated with 0.005 μg conjugate per well. Subsequently, plates were blocked with 1% ovalbumin in PBS-T (PBS with 0.05% [vol/vol] Tween 20) for 1 h at 20°C with shaking. After washing with PBS-T, a volume of 60 μl of sample and 60 μl of primary antibody was added and incubated for 90 min at 20°C with shaking. Final antibody dilutions were 1:6,500 for ST:G8, 1:16,000 for clone 29, and 1:30,000 for clone 30. The plates were then washed with PBS-T and incubated at room temperature for 1 h with 100 μl anti-mouse secondary antibody diluted in PBS-T (ST:G8, 1:400; clones 29 and 30, 1:2,000). After a final wash, the plates were developed with 100 μl developing buffer for 15 to 20 min, development was stopped by the addition of 50 μl 2 M NaOH, and the OD_{405} was measured.

The competitive ELISA using the anti-STp clone 31 MAb was performed by using a different coating approach. ELISA plates (Nunc CovaLink) were coated with synthetic STp according to the manufacturer's instructions. Briefly, 50 μl of 1 μM STp in PBS was mixed with 50 μl of an EDC solution [184 μg bis(sulfosuccinimidyl)suberate (BS3) and 50 mg EDC in PBS] and added to all wells, and the wells were incubated overnight at 20°C. The ELISA was then performed with washing steps, blocking steps, and development as described above. The final concentration of clone 31 primary antibody was 1:16,000, and that of anti-mouse secondary antibody was 1:500.

The ETEC and synthetic STh and STp peptides had similar antigenic properties in all ELISAs, and for each ELISA, at least one experiment was performed by using ETEC STh and STp.

Cloning and expression of proguanylin and prouroguanylin. The proforms of guanylin and uroguanylin were chosen as coatings for guanylin and uroguanylin competitive ELISAs to ensure binding and competition of A-form-specific antibodies (48). The cDNA sequences of proguanylin (IMAGE ID 100062076) and prouroguanylin (IMAGE ID 7939624; http://www.imageconsortium.org) were cloned into the pSXG vector (49) as GST fusions. Standard protocols were used (50). The two sequences were amplified by PCR with the mutagenic primers listed in Table 1. This introduced EcoRI and BamHI restriction sites on each end of the PCR products. The PCR products and the empty pSXG vector were subsequently digested with EcoRI and BamHI, and these were ligated, resulting in in-frame fusions of the GST coding sequence (CDS) and the proguanylin and prouroguanylin CDSs, respectively. The resulting plasmid carrying the proguanylin sequence was named pSXG-ProG-GN, and the one carrying the prouroguanylin sequence was named pSXG-ProU-UGN. Due to the expression of insoluble protein from plasmid pSXG-ProU-UGN, an additional plasmid, pSXG-ProG-UGN, was constructed by replacing the mature peptide-encoding sequence of guanylin in the pSXG-ProG-GN vector with the peptide-encoding sequence of uroguanylin. Plasmid pSXG-ProU-UGN was used as the template in a PCR using the primers listed in Table 1. The resulting PCR product contained the sequence of the uroguanylin peptide and a part of the pSXG vector flanked by the restriction sites BbvCI and AatII. The PCR product and the pSXG-ProG-GN vector were then both digested with BbvCI and AatII and subsequently ligated. All plasmids were verified by sequencing.

The GST-proguanylin-guanylin (GST-ProG-GN) and GST-proguanylin-uroguanylin (GST-ProG-UGN) fusion proteins were expressed from plasmids pSXG-ProG-GN and pSXG-ProG-UGN, respectively, us-

TABLE 1 PCR primers used to construct GST-ProG-GN, GST-ProU-UGN, and GST-ProG-UGN

Primer (restriction site)	Sequence (5′–3′)	Purpose
Guanylin Fwd (EcoRI)	GCCTTGGCAGAATTCGTCACCGTGCAG	Cloning of the ProG-GN sequence into plasmid pSXG
Guanylin Rev (BamHI)	TGGGCCCATGGATCCTTAGCATCCGGT	Cloning of the ProG-GN sequence into plasmid pSXG
Uroguanylin Fwd (EcoRI)	GCAGAGCACAGAATTCGTCTACATCCAGTACC	Cloning of the ProU-UGN sequence into plasmid pSXG
Uroguanylin Rev (BamHI)	TGGGCGGATCCTACCCAGGGCTATCTCA	Cloning of the ProU-UGN sequence into plasmid pSXG
ProG-BbvCl-Uroguanylin	CGCTGAGGACAACGACGACTGTGAGCTGTGTGTGAAC	Cloning of the UGN peptide sequence into plasmid pSXG-ProG
pSXG-far-right	GGTTCCGCGCACATTTCCCCGAAAAGTG	Cloning of the UGN peptide sequence into plasmid pSXG-ProG

ing *E. coli* Origami B cells (Novagen/Merck, Darmstadt, Germany). Transformations and inoculations were performed according to the manufacturer's instructions, and the bacteria were grown in 500-ml cultures of LB medium supplemented with appropriate antibiotics at 37°C. At an OD_{600} of 0.5, protein expression was induced by the addition of isopropyl-β-D-thiogalactopyranoside (IPTG) to a final concentration of 400 μM. The cultures were incubated for an additional 3 to 4 h at 37°C before they were harvested by centrifugation at 17,000 × *g* for 10 min at 4°C. The pellets were resuspended in 10 ml PBS buffer with 200 mM NaCl and lysed by sonication. Samples were subsequently centrifuged in Corex tubes at 48,000 × *g* for 20 min at 4°C, and supernatants were transferred into clean 15-ml tubes. The GST-tagged proteins were purified by using 1 ml of a 50% glutathione-Sepharose 4B slurry (GE Healthcare, Little Chalfont, United Kingdom) per sample, according to the manufacturer's instructions. The elution step was repeated three times. Purified fusion proteins were examined by SDS-PAGE using 12% slab gels. Both pSXG-ProG-GN and pSXG-ProG-UGN showed a single prominent band at a molecular mass of 38 kDa, and Western blots with antiguanylin and antiuroguanylin antibodies confirmed the identities of the fusion proteins. Protein concentrations were estimated by measuring the absorbance at 280 nm.

Competitive guanylin and uroguanylin ELISAs. Competitive guanylin and uroguanylin ELISAs were developed based on a standard protocol from the antibody supplier (Abcam), and coating steps were performed according to the plate manufacturer's instructions. ELISA plates (Nunc Immobilizer glutathione) were coated with 100 μl GST-tagged fusion proteins (50 nM GST-ProG-UGN and 25 nM GST-ProG-GN) per well in PBS (104.7 mM NaCl, 10.6 mM Na_2HPO_4, 2.9 mM KH_2PO_4 [pH 7.2]) and incubated overnight at 4°C. The plates were subsequently washed and blocked for 1 h with PBS-T at 20°C with shaking. After washing, 55 μl of sample was mixed with 55 μl of primary antibody solution (final dilutions in PBS-T of 1:1,000 for antiuroguanylin and 1:4,000 for antiguanylin), added to each well, and incubated for 90 min at 20°C with shaking. After washing, 100 μl secondary antibody diluted in PBS-T (final dilution 1:400 of anti-goat for antiuroguanylin and 1:400 of anti-rabbit for antiguanylin) was added per well, followed by incubation at 20°C for 1 h. After washing, the plates were developed with 100 μl developing buffer for 30 to 40 min, development was stopped by the addition of 50 μl 2 M NaOH, and the OD_{405} was read.

Statistical and regression analyses. The R statistical computing environment was used for statistical and regression analyses (http://www.r-project.org/). Analysis of variance (ANOVA) and Tukey's honestly significant difference test were used to evaluate whether the abilities of the individual peptides to inhibit binding to ELISA coatings in the polyclonal ELISAs were significantly different ($P < 0.05$). To calculate the half-maximal inhibitory concentration (IC_{50}) in the monoclonal antibody ST:G8 ELISA and the EC_{50} in the T-84 cell assay, four-parameter log-logistic regression was performed by using the drc R package (51). For IC_{50} calculations, all peptides were assumed to have the same minimum, and for EC_{50} calculations, the maximum values and slopes were also assumed to be the same. Relative IC_{50}s and their significances were calculated with the drc selectivity index (SI) function.

RESULTS

Molecular dynamics of STh and the endogenous GC-C ligands. To assess the structural similarity between STh and the endogenous ligands, we constructed a structural model for STh based on the available experimental structures of STp, guanylin, and uroguanylin. This model and the experimental structures of guanylin and uroguanylin were subjected to molecular dynamics (MD) simulations for a thorough assessment of structural similarity. All molecules in the simulations contained the full-length peptides, including the reportedly unstructured N termini. The simulations confirmed that the N termini indeed seem to be unstructured, and hence, evaluation of structural similarity was restricted to the backbone of the 12-amino-acid region from the first to the last shared cysteines. The final structures, resulting from the simulations, had the following RMSD values: 0.8 Å for guanylin/uroguanylin, 2.4 Å for STh/guanylin, and 2.6 Å for STh/uroguanylin. In a follow-up MD experiment, we assessed the structural effect of the ST-specific disulfide bridge by making a model where this bridge was broken (STh-2SS). Interestingly, this made the backbone of STh more similar to those of the endogenous peptides, as reflected by RMSD values of 0.9 Å for STh-2SS/guanylin and 0.7 Å for STh-2SS/uroguanylin. This suggests that the ST-specific disulfide bridge not only locks ST in the active form but also changes the backbone structure slightly compared to the structure of the endogenous ligands.

The structural similarities of the GC-C ligand peptide backbones imply that the same residues in equivalent positions may contribute to similar epitopes. Figure 1 shows structural models and a sequence alignment for all four GC-C ligands with residues shared by at least three peptides highlighted. The shared residues form structural clusters that warrant experimental exploration of possible similar epitopes.

STh, STp, guanylin, and uroguanylin peptides have expected masses and correct numbers of disulfide bridges and are biologically active. To ensure relevant results on possible similar epitopes, the use of GC-C ligand peptides that are both structurally intact and biologically active is vital. To assess structural integrity, we investigated the presence of disulfide bridges by mass spectrometric analysis (Table 2). The peptides were analyzed in their native state and in a reduced form where bridge reformation was prevented by alkylation. The native peptides displayed monoisotopic peaks that corresponded to the expected masses of the native peptides with intact disulfide bridges, and the reduced and alkylated controls showed the expected masses. These results strongly suggest that the peptides are structurally intact. The biological activity of all four peptides was confirmed by using a T-84 cell assay, and the observed EC_{50}s were 58 ± 9 nM for ETEC STh,

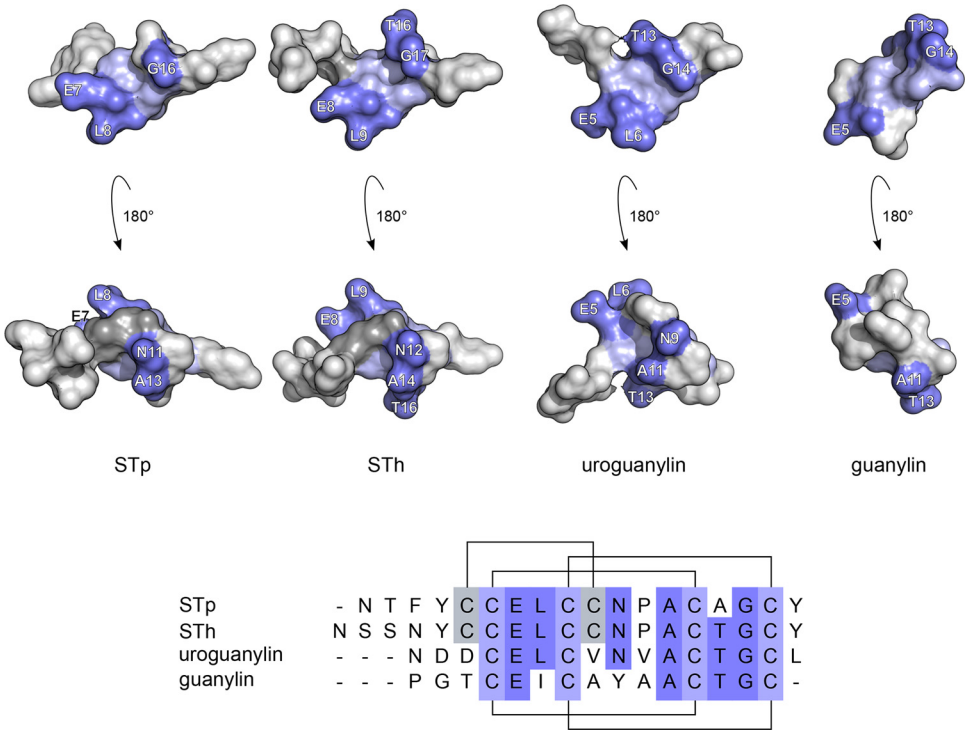

FIG 1 Structure and sequence comparisons of STp, STh, uroguanylin, and guanylin. (A) Surface representation of structural models of STp and STh and experimental structures of uroguanylin (PDB accession no. 1UYA) and guanylin (PDB accession no. 1GNA). The shared cysteines are shown in light blue, other residues shared by at least three of the peptides are in dark blue, and the ST-specific disulfide bridge is in dark gray. Each structure is shown from two opposite sides. (B) Sequence alignment of STp, STh, uroguanylin, and guanylin, colored as described above for the structures. The ST disulfide bonding pattern is shown above the alignment, and the (uro)guanylin pattern is shown below.

44 ± 6 nM for ETEC STp, 79 ± 10 nM for synthetic STh, 161 ± 26 nM for synthetic STp, 692 ± 101 nM for guanylin, and 174 ± 21 nM for uroguanylin.

All six anti-ST antibodies have neutralizing capacity. For an ST vaccine to be successful, elicited antibodies should have the ability to neutralize the biological activity of ST. The neutralizing capability of the anti-ST antibodies used in this study was assessed by using a T-84 cell assay by preincubating the ST peptide with the various antibodies before biological activity was assessed. The anti-STh and anti-STp polyclonal antibodies, but not the control antibodies, were able to neutralize STh (Fig. 2A) and STp (data not shown). The anti-STp MAbs clone 29, clone 30, and clone 31 neutralized STp (Fig. 2B). Clone 29 and clone 30 also neutralized STh (data not shown), in contrast to clone 31, which neutralized only STp (Fig. 3). To our knowledge, this is the first report of an anti-ST antibody that selectively neutralizes only one variant of ST. The reported neutralizing capacity of anti-STh MAb ST:G8 against both STh and STp was confirmed (data not shown).

TABLE 2 Theoretical and observed masses of GC-C ligand peptides

Peptide	Mass (Da)				
	Theoretical			Observed[a]	
	Native	Reduced	Reduced and alkylated	Native	Reduced and alkylated
STh[b]	2,042.3	2,048.3	2,390.5	2,041.6	2,389.8
STp[b]	1,972.3	1,978.3	2,320.5	1,971.7	2,319.9
Uroguanylin	1,667.9	1,671.9	1,900.0	1,667.7	1,899.8
Guanylin	1,458.7	1,462.7	1,690.8	1,458.6	1,690.6

[a] Observed monoisotopic peaks in mass spectrometry. All peptides bound Na^+ and/or K^+ to some degree. The reported masses are without binding of ions.
[b] Synthetic STh and STp peptides had the same observed masses as those of peptides purified from ETEC.

The GC-C ligand peptides have similar epitopes. To evaluate the presence of similar epitopes in STh, STp, uroguanylin, and guanylin, we analyzed the peptides in four different competitive ELISAs, based on polyclonal antibodies against STh, STp, uroguanylin, and guanylin, respectively (Fig. 4). In the STh ELISA (Fig. 4A), guanylin did not inhibit the binding of the anti-STh antibody to the STh-ovalbumin coating and acted as a negative control. The STh and STp peptides both approached a maximum inhibition of 75% at high peptide concentrations, whereas uroguanylin showed a maximum inhibition of 20%. All values were significantly different ($P < 0.0001$) from those of the control. This suggests that all STh epitopes are shared with STp but that only a fraction (27%) of them have similar counterparts in uroguanylin. In the STp ELISA (Fig. 4B), neither uroguanylin nor guanylin displayed any inhibition, and guanylin was chosen as a negative control. STp approached a maximum inhibition of 80%, and STh approached 65% inhibition, both of which were significantly different ($P < 0.0001$) from the values for the control. This suggests that there are STp-specific epitopes that are not shared with STh. The last two ELISAs, developed for uroguanylin and guanylin, also showed cross-reactivity. STh inhibited 20% of antiuroguanylin antibody binding, which was significantly different ($P < 0.0001$) from the value for the negative control guanylin (Fig. 4C). STp approached

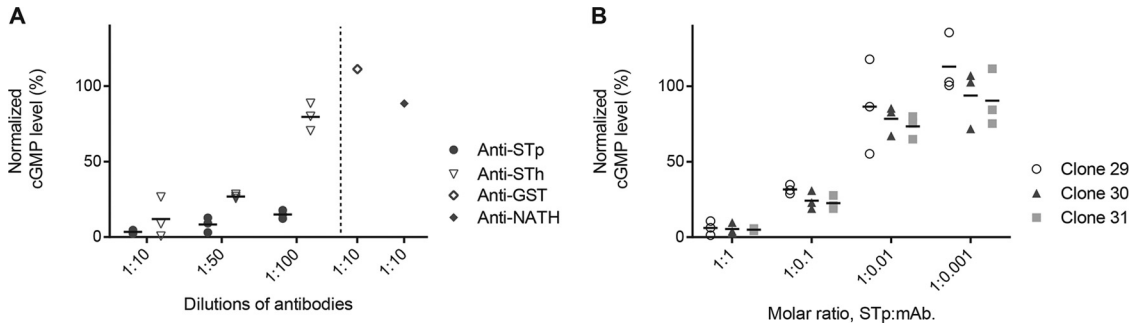

FIG 2 Anti-ST antibodies neutralize ST-induced intracellular cGMP production in the T-84 cell assay. (A) Ten nanograms of STh was preincubated with different dilutions of polyclonal anti-STh and anti-STp antibodies (horizontal axis) prior to the T-84 cell assay. Normalized cGMP levels are given as percentages of the positive control containing only STh peptide (vertical axis). Two unrelated polyclonal antibodies were included as negative controls. (B) Ten nanograms of STp was preincubated with different molar ratios of three anti-STp monoclonal antibodies, clone 29, clone 30, and clone 31 (horizontal axis), prior to the T-84 cell assay. Normalized cGMP levels are given as percentages of the positive control containing only STp peptide (vertical axis). The results from three independent experiments are shown, with the means shown as horizontal lines.

10% inhibition but was not significantly different from the control. In the guanylin ELISA, both STh and uroguanylin approached 15% inhibition, which was significantly different ($P < 0.0001$) from the value of the negative control STp (Fig. 4D). This suggests that STh shares similar epitopes with uroguanylin and that STh and uroguanylin share similar epitopes with guanylin. Interestingly, the degree of shared similar epitopes seems to correlate well with sequence identities (Fig. 4). In conclusion, the four ELISAs demonstrate that the GC-C ligand peptides have similar epitopes and that cross-reactivity may occur upon vaccination with an ST vaccine.

Neutralizing anti-STh MAb cross-reacts with uroguanylin. To investigate similar epitopes further, we analyzed the possible cross-reactivities of one anti-STh and three anti-STp MAbs. In the anti-STh ST:G8 ELISA, STh, STp, and uroguanylin, but not guanylin, inhibited the binding of the MAb to the STh-ovalbumin ELISA coating (Fig. 5). However, the half-maximal inhibitory concentrations (IC_{50}s) for STp and uroguanylin were 4.2-fold (±0.3-fold) ($P < 0.0001$) and 73-fold (±7-fold) ($P < 0.0001$) lower, respectively, than that for STh. This suggests that the epitopes recognized by the ST:G8 MAb are not identical in the three peptides. The observed differences in affinity correlate well with sequence identity (Fig. 4A).

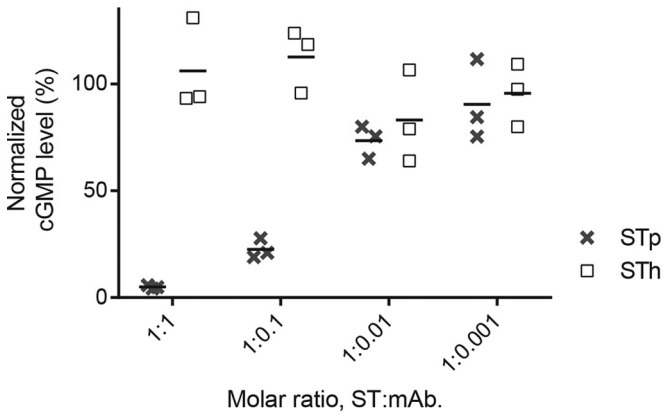

FIG 3 Anti-STp monoclonal antibody clone 31 specifically neutralizes induction of intracellular cGMP production mediated by STp but not by STh in the T-84 cell assay. Ten nanograms of STp and 10 ng of STh were preincubated with different molar ratios of clone 31 (horizontal axis) prior to the T-84 cell assay. Normalized cGMP levels are given as percentages of the positive control containing only STp peptide (vertical axis). The results from three independent experiments are shown, with the means shown as horizontal lines.

Three neutralizing anti-STp MAbs do not cross-react with endogenous peptides. In the three anti-STp MAb ELISAs, no cross-reactivity to the endogenous peptides was observed (data not shown). This demonstrates that it is possible to obtain antibodies that neutralize ST and do not cross-react. The ELISAs also confirmed the apparent STp specificity of clone 31, which was observed in the T-84 cell neutralization experiments (Fig. 3), as STh was not able to inhibit the binding of clone 31 to an STp-based ELISA coating. When developing the ELISA for clone 31, we initially attempted to use STh-ovalbumin coating, which was successfully used for the other three MAbs, but clone 31 did not bind to that coating. Clone 31 also bound poorly to STp-ovalbumin conjugates when the N terminus of STp was targeted in the conjugation reaction. However, when STp was conjugated to ELISA plates via its C-terminal and glutamate 7 carboxyl groups, leaving the N terminus of STp exposed, good binding was obtained, and a sensitive ELISA could be developed. This indicates that the N terminus of STp may be part of the clone 31 epitope.

DISCUSSION

Cross-reactivity between antibodies against ST and the (uro)guanylin peptides has been a concern for ST vaccine development since the discovery of these endogenous peptides two decades ago (1, 2, 9). In this study, we have demonstrated that the GC-C ligand peptides have similar epitopes and that immunological cross-reactivity is a potential obstacle to the development of an ST-based vaccine.

The two ST polyclonal antibodies displayed different ST-cross-reacting properties: the anti-STh antibody seemed to recognize both STh and STp to a similar extent (Fig. 4A), whereas a subset of the anti-STp antibodies seemed be specific for STp (Fig. 4B). The two ST peptides have a 15-amino-acid shared region from the first to the last tyrosines, with only one amino acid difference, namely, the STh threonine residue (STh-T16), which is alanine in STp (STp-A15). Similar epitopes are likely to be located in this region. The results obtained with the anti-STh antibody suggest either that the STh-T16 residue is not part of any epitope or that an

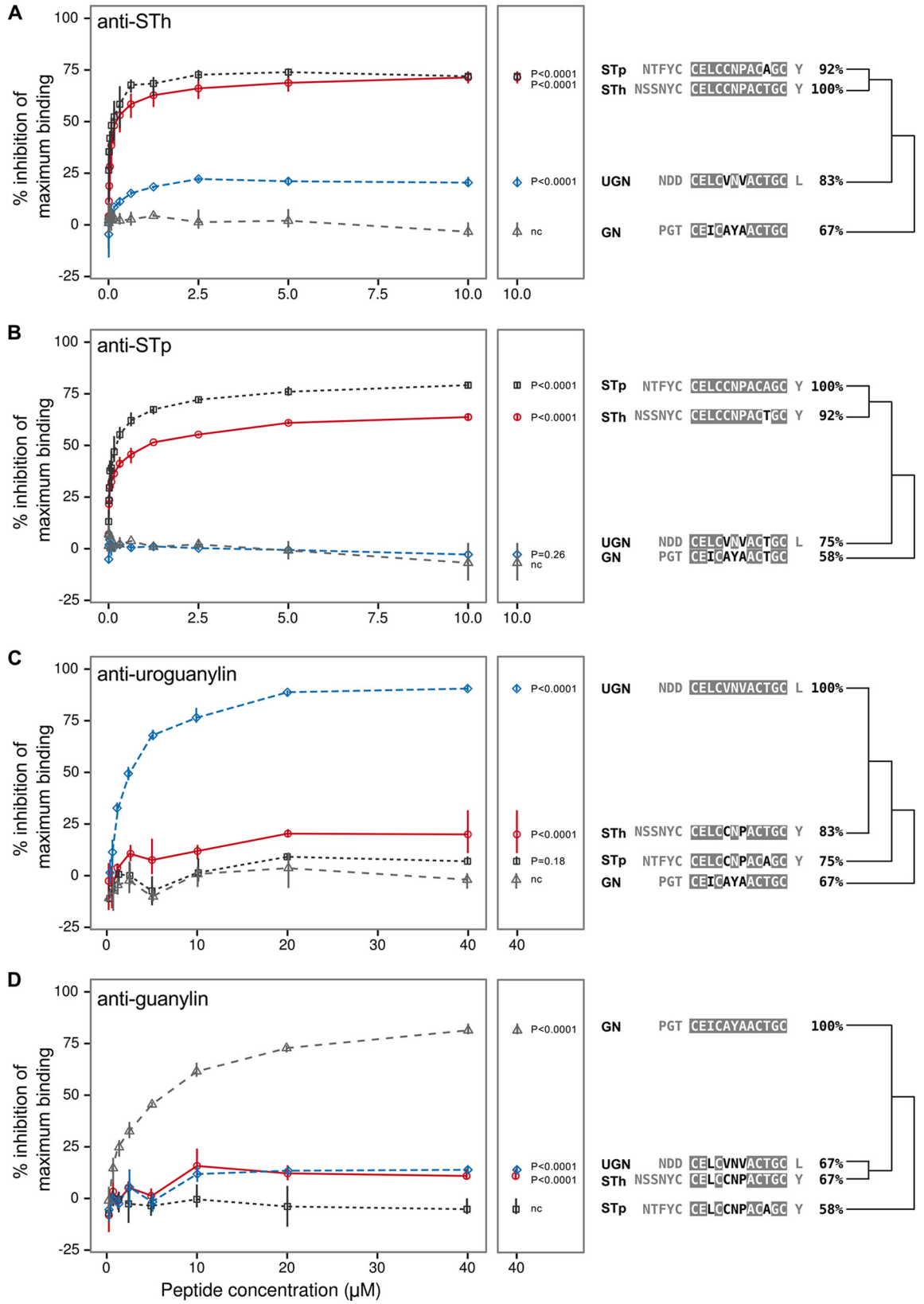

FIG 4 Anti-STh (A), anti-STp (B), antiuroguanylin (C), and antiguanylin (D) polyclonal antibodies were tested for their abilities to bind to the STh, STp, uroguanylin (UGN), and guanylin (GN) peptides in competitive ELISAs. Each panel to the left displays data from three independent experiments where serial dilutions of the four peptides (horizontal axis) were tested in triplicate. Points represent the means of all three experiments, and the vertical lines outline the maximum and minimum values. The vertical axis represents the ability of the peptides to inhibit the binding of antibody to the ELISA coating, given as a percentage of maximum binding (activity) measured in the absence of a competing peptide. The middle panels repeat the mean values of the highest peptide doses, along with *P* values for comparisons of the test peptides and the negative control (nc). Sequence alignments are shown to the right of the panels, where the GC-C ligand domain residues are shaded to indicate identity to those of the cognate peptide for each antibody. The sequence identities are given, and the dendrograms reflect similarities.

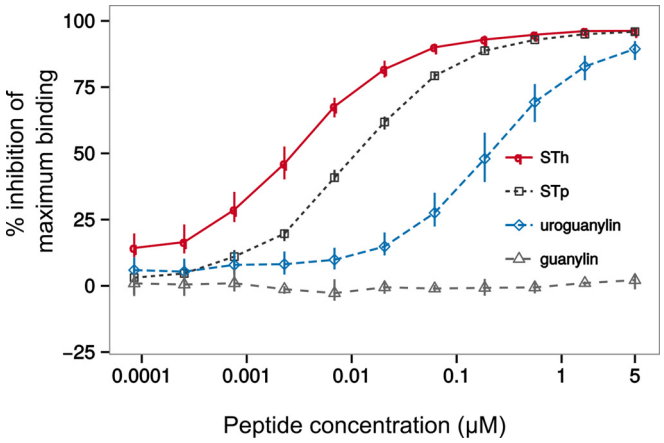

FIG 5 Competitive ELISA to estimate the abilities of STh, STp, uroguanylin, and guanylin peptides to bind to the anti-STh ST:G8 monoclonal antibody. Three independent experiments were performed with serial dilutions of all peptides in triplicate (horizontal axis; logarithmic scale). Points represent the means of all three experiments, and the vertical lines outline the maximum and minimum values. The vertical axis represents the ability of the peptides to inhibit the binding of antibody to the ELISA coating, given as a percentage of maximum binding (activity) measured in the absence of a competing peptide. The maximum inhibition values calculated by regression analysis from these data are 97% ± 1% for STh, 95% ± 1% for STp, and 94% ± 2% for uroguanylin. Calculated half-maximal inhibitory concentrations (IC_{50}s) are 0.0027 ± 0.0001 μM for STh, 0.0120 ± 0.0006 μM for STp, and 0.21 ± 0.01 μM for uroguanylin.

alanine residue in this position does not interfere with binding. The latter possibility cannot be excluded, as alanine is a smaller amino acid than threonine. Interestingly, the difference in this position may also explain the existence of STp-specific epitopes. Since threonine both is larger than alanine and contains a hydroxyl group, it is possible that binding to an epitope involving STp-A15 may be disrupted by threonine. An alternative explanation is that the STp-specific epitopes are located at the N terminus, which harbors three unique N-terminal residues.

Cross-reaction to uroguanylin was observed with the anti-STh polyclonal antibody but not the anti-STp polyclonal antibody (Fig. 4A and B). The most likely explanation for this is that uroguanylin is more similar to STh than STp, due to uroguanylin sharing the STh-T16 residue (Fig. 1). This is as expected from the sequence similarities and is supported by the uroguanylin and guanylin ELISA results (Fig. 4C and D), where a larger subset of the antiuroguanylin and antiguanylin polyclonal antibodies cross-reacted with STh than with STp. Interestingly, the anti-STh antibody did not cross-react with guanylin despite the fact that it also shares the STh-T16 residue. As the STh residues L9 and N12 are the only residues that are uniquely shared with uroguanylin, it is likely that either or both of these residues contribute to the STh epitopes that have similar counterparts in uroguanylin.

The anti-STh ST:G8 MAb cross-reacted with both STp and uroguanylin but with 4.4-fold- and 73-fold-lower affinities, respectively (Fig. 5). This suggests that the epitopes recognized in each of the three peptides are similar but not identical and that they, at least in part, are located in the GC-C ligand domain. Hence, differences in amino acids in the GC-C ligand domain may explain the different IC_{50} values. The 4.4-fold difference in IC_{50}s between STh and STp may thus be explained by the STh-T16/STp-A15 difference and suggests that STh-T16 is part of the ST:G8 epitope. The small size and missing hydroxyl group of alanine compared to threonine seems to be compatible with MAb binding but leads to a lower affinity. Uroguanylin shares the STh-T16 residue but has an even lower affinity for ST:G8 than STp, reflected by the 73-fold-lower IC_{50} value than that for STh. Hence, the difference in affinity is likely due to other amino acid differences or structural differences of the backbone. Inside the GC-C ligand domain, the differing residues are V8 and V10 of uroguanylin, which correspond to C11 and P13 of STh, respectively. In addition, STp shares STh residues Y5, C6, and Y19, which are different in uroguanylin and may thus also be part of the epitope. The ST:G8 MAb did not cross-react with guanylin, a property shared with the polyclonal anti-STh antibody, thus implicating either or both STh residues L9 and N12 as also being potential ST:G8 epitope residues.

It is striking that only antibodies raised against STh cross-reacted with uroguanylin (Fig. 4A and 5) and that neither anti-STh nor anti-STp antibodies showed any cross-reaction to guanylin (Fig. 4A and B and 5). Since guanylin is the least similar to ST of the two endogenous peptides, it is perhaps not surprising that cross-reactivity was observed only for uroguanylin. The finding that only STh-based immunogens, and not STp, give rise to cross-reacting antibodies is more surprising. The hypothesis that STh-T16 is involved in cross-reactivity is supported by the two anti-STp MAbs clone 29 and clone 30, which both recognized STh but not uroguanylin. The clone 31 MAb, on the other hand, is specific for STp, which suggests that the apparently unstructured N-terminal residues may also be part of epitopes.

An efficient ST-based vaccine should elicit a strong immune response with neutralizing capability. All six anti-ST antibodies tested in this study neutralized STh and STp, except for MAb clone 31, which neutralized only STp. To avoid cross-reactivity to the endogenous peptides, it is tempting to suggest that vaccines should be based on STp rather than STh. Another option could be to base the vaccine on an STh-T16A mutant, which would make STh identical to STp in the toxic domain but leave the N terminus intact. Such a vaccine molecule may escape the problem of cross-reactivity while at the same time exposing potentially important STh-specific N-terminal epitopes. The MD simulations suggested that the ST-specific disulfide bridge contributes to making the backbone structure of the STh GC-C ligand domain subtly different from those of the endogenous peptides. Hence, making sure that all disulfide bridges are intact in an ST vaccine not only may be important to ensure the proper presentation of structural epitopes but also may reduce the risk of cross-reactivity.

The presence of similar epitopes on STh and uroguanylin raises concerns that an ST-based vaccine may induce autoimmune reactions and interference with GC-C-mediated signaling. However, the immune system has protective mechanisms that limit the production of antibodies against self-antigens. Such immunological tolerance may reduce cross-reactivity but may also inhibit an efficient anti-ST immune response upon vaccination. Hence, it may be important to avoid epitopes that are shared with the endogenous peptides, both to minimize the risk of cross-reactivity and to optimize the immune response to an ST-based vaccine.

In conclusion, we have demonstrated that immunological cross-reactivity with the endogenous GC-C ligand peptides is a potential obstacle to ST vaccine development. However, the partial nature and low affinity of the observed cross-reactions suggest that the risk of adverse effects from a future ST vaccine may be low.

Furthermore, the results presented here suggest that it should be possible to circumvent this problem by either basing the vaccine on STp or carefully selecting appropriate mutations in STh to disrupt epitopes shared with the endogenous peptides. Even a vaccine with a low risk of immunological cross-reactivity may cause unacceptable levels of adverse events when introduced to a large population. Hence, it is of paramount importance for the development of a safe ST vaccine that its design includes strategies to avoid cross-reactivity.

ACKNOWLEDGMENTS

We thank Dag Helland for useful discussions; John D. Clements and Sandhya S. Visweswariah for discussions and for providing laboratory reagents; and Thomas A. Aloysius, Marie-Josée Porcheron, and Elisabeth Silden for their skilled technical assistance.

The research leading to these results has received funding from the Research Council of Norway (GLOBVAC program, grant no. 185872-EntVac), PATH (grant no. 102290-002), and the European Union Seventh Framework Program for research, technological development, and demonstration under grant agreement no. 261472-STOPENTERICS. A.M.T. was supported by the University of Bergen.

REFERENCES

1. **Walker RI, Steele D, Aguado T.** 2007. Analysis of strategies to successfully vaccinate infants in developing countries against enterotoxigenic E. coli (ETEC) disease. Vaccine **25:**2545–2566. http://dx.doi.org/10.1016/j.vaccine.2006.12.028.
2. **Taxt A, Aasland R, Sommerfelt H, Nataro J, Puntervoll P.** 2010. Heat-stable enterotoxin of enterotoxigenic Escherichia coli as a vaccine target. Infect. Immun. **78:**1824–1831. http://dx.doi.org/10.1128/IAI.01397-09.
3. **Liu M, Ruan X, Zhang C, Lawson SR, Knudsen DE, Nataro JP, Robertson DC, Zhang W.** 2011. Heat-labile- and heat-stable-toxoid fusions (LTR192G-STaP13F) of human enterotoxigenic Escherichia coli elicit neutralizing antitoxin antibodies. Infect. Immun. **79:**4002–4009. http://dx.doi.org/10.1128/IAI.00165-11.
4. **Zhang W, Zhang C, Francis DH, Fang Y, Knudsen D, Nataro JP, Robertson DC.** 2010. Genetic fusions of heat-labile (LT) and heat-stable (ST) toxoids of porcine enterotoxigenic Escherichia coli elicit neutralizing anti-LT and anti-STa antibodies. Infect. Immun. **78:**316–325. http://dx.doi.org/10.1128/IAI.00497-09.
5. **Zeng W, Azzopardi K, Hocking D, Wong CY, Robevska G, Tauschek M, Robins-Browne RM, Jackson DC.** 2012. A totally synthetic lipopeptide-based self-adjuvanting vaccine induces neutralizing antibodies against heat-stable enterotoxin from enterotoxigenic Escherichia coli. Vaccine **30:**4800–4806. http://dx.doi.org/10.1016/j.vaccine.2012.05.017.
6. **Deng G, Zeng J, Jian M, Liu W, Zhang Z, Liu X, Wang Y.** 2013. Nanoparticulated heat-stable (STa) and heat-labile B subunit (LTB) recombinant toxin improves vaccine protection against enterotoxigenic Escherichia coli challenge in mouse. J. Biosci. Bioeng. **115:**147–153. http://dx.doi.org/10.1016/j.jbiosc.2012.09.009.
7. **Ruan X, Robertson DC, Nataro JP, Clements JD, Zhang W.** 2014. Characterization of heat-stable (STa) toxoids of enterotoxigenic Escherichia coli fused to a double mutant heat-labile toxin peptide in inducing neutralizing anti-STa antibodies. Infect. Immun. **82:**1823–1832. http://dx.doi.org/10.1128/IAI.01394-13.
8. **Kotloff KL, Nataro JP, Blackwelder WC, Nasrin D, Farag TH, Panchalingam S, Wu Y, Sow SO, Sur D, Breiman RF, Faruque AS, Zaidi AK, Saha D, Alonso PL, Tamboura B, Sanogo D, Onwuchekwa U, Manna B, Ramamurthy T, Kanungo S, Ochieng JB, Omore R, Oundo JO, Hossain A, Das SK, Ahmed S, Qureshi S, Quadri F, Adegbola RA, Antonio M, Hossain MJ, Akinsola A, Mandomando I, Nhampossa T, Acácio S, Biswas K, O'Reilly CE, Mintz ED, Berkeley LY, Muhsen K, Sommerfelt H, Robins-Browne RM, Levine MM.** 2013. Burden and aetiology of diarrhoeal disease in infants and young children in developing countries (the Global Enteric Multicenter Study, GEMS): a prospective, case-control study. Lancet **382:**209–222. http://dx.doi.org/10.1016/S0140-6736(13)60844-2.
9. **Wolf MK.** 1997. Occurrence, distribution, and associations of O and H serogroups, colonization factor antigens, and toxins of enterotoxigenic Escherichia coli. Clin. Microbiol. Rev. **10:**569–584.
10. **Steinsland H, Valentiner-Branth P, Perch M, Dias F, Fischer TK, Aaby P, Mølbak K, Sommerfelt H.** 2002. Enterotoxigenic Escherichia coli infections and diarrhea in a cohort of young children in Guinea-Bissau. J. Infect. Dis. **186:**1740–1747. http://dx.doi.org/10.1086/345817.
11. **Lockwood DE, Robertson DC.** 1984. Development of a competitive enzyme-linked immunosorbent assay (ELISA) for Escherichia coli heat-stable enterotoxin (STa). J. Immunol. Methods **75:**295–307. http://dx.doi.org/10.1016/0022-1759(84)90113-3.
12. **Takeda T.** 1983. Neutralization of activity of two different heat-stable enterotoxins (STh and STp) of enterotoxigenic *Escherichia coli* by homologous and heterologous antisera. FEMS Microbiol. Lett. **20:**357–359. http://dx.doi.org/10.1111/j.1574-6968.1983.tb00147.x.
13. **Aref N-EM, Saeed AM.** 2011. Design and characterization of highly immunogenic heat-stable enterotoxin of enterotoxigenic Escherichia coli K99(+). J. Immunol. Methods **366:**100–105. http://dx.doi.org/10.1016/j.jim.2011.01.012.
14. **Kennedy DJ, Greenberg RN, Dunn JA, Abernathy R, Ryerse JS, Guerrant RL.** 1984. Effects of Escherichia coli heat-stable enterotoxin STb on intestines of mice, rats, rabbits, and piglets. Infect. Immun. **46:**639–643.
15. **Kaper JB, Nataro JP, Mobley HL.** 2004. Pathogenic Escherichia coli. Nat. Rev. Microbiol. **2:**123–140. http://dx.doi.org/10.1038/nrmicro818.
16. **Forte LR.** 2004. Uroguanylin and guanylin peptides: pharmacology and experimental therapeutics. Pharmacol. Ther. **104:**137–162. http://dx.doi.org/10.1016/j.pharmthera.2004.08.007.
17. **Hamra FK, Forte LR, Eber SL, Pidhorodeckyj NV, Krause WJ, Freeman RH, Chin DT, Tompkins JA, Fok KF, Smith CE, Duffin KL, Siegel NR, Currie MG.** 1993. Uroguanylin: structure and activity of a second endogenous peptide that stimulates intestinal guanylate cyclase. Proc. Natl. Acad. Sci. U. S. A. **90:**10464–10468. http://dx.doi.org/10.1073/pnas.90.22.10464.
18. **Ozaki H, Sato T, Kubota H, Hata Y, Katsube Y, Shimonishi Y.** 1991. Molecular structure of the toxin domain of heat-stable enterotoxin produced by a pathogenic strain of Escherichia coli. A putative binding site for a binding protein on rat intestinal epithelial cell membranes. J. Biol. Chem. **266:**5934–5941.
19. **Marx UC, Klodt J, Meyer M, Gerlach H, Rösch P, Forssmann WG, Adermann K.** 1998. One peptide, two topologies: structure and interconversion dynamics of human uroguanylin isomers. J. Pept. Res. **52:**229–240.
20. **Skelton NJ, Garcia KC, Goeddel DV, Quan C, Burnier JP.** 1994. Determination of the solution structure of the peptide hormone guanylin: observation of a novel form of topological stereoisomerism. Biochemistry **33:**13581–13592. http://dx.doi.org/10.1021/bi00250a010.
21. **Schulz A, Marx UC, Tidten N, Lauber T, Hidaka Y, Adermann K.** 2005. Side chain contributions to the interconversion of the topological isomers of guanylin-like peptides. J. Pept. Sci. **11:**319–330. http://dx.doi.org/10.1002/psc.625.
22. **Nakazato M.** 2001. Guanylin family: new intestinal peptides regulating electrolyte and water homeostasis. J. Gastroenterol. **36:**219–225. http://dx.doi.org/10.1007/s005350170106.
23. **Sindić A, Schlatter E.** 2006. Cellular effects of guanylin and uroguanylin. J. Am. Soc. Nephrol. **17:**607–616. http://dx.doi.org/10.1681/ASN.2005080818.
24. **Nakazato M, Yamaguchi H, Kinoshita H, Kangawa K, Matsuo H, Chino N, Matsukura S.** 1996. Identification of biologically active and inactive human uroguanylins in plasma and urine and their increases in renal insufficiency. Biochem. Biophys. Res. Commun. **220:**586–593. http://dx.doi.org/10.1006/bbrc.1996.0447.
25. **Moss NG, Fellner RC, Qian X, Yu SJ, Li Z, Nakazato M, Goy MF.** 2008. Uroguanylin, an intestinal natriuretic peptide, is delivered to the kidney as an unprocessed propeptide. Endocrinology **149:**4486–4498. http://dx.doi.org/10.1210/en.2007-1725.
26. **Qian X, Moss NG, Fellner RC, Goy MF.** 2008. Circulating prouroguanylin is processed to its active natriuretic form exclusively within the renal tubules. Endocrinology **149:**4499–4509. http://dx.doi.org/10.1210/en.2007-1724.
27. **Jaleel M.** 2002. Expression of the receptor guanylyl cyclase C and its ligands in reproductive tissues of the rat: a potential role for a novel signaling pathway in the epididymis. Biol. Reprod. **67:**1975–1980. http://dx.doi.org/10.1095/biolreprod.102.006445.
28. **Gong R, Ding C, Hu J, Lu Y, Liu F, Mann E, Xu F, Cohen MB, Luo M.** 2011. Role for the membrane receptor guanylyl cyclase-C in attention

deficiency and hyperactive behavior. Science **333:**1642–1646. http://dx.doi.org/10.1126/science.1207675.
29. **Schonberger LB, Bregman DJ, Sullivan-Bolyai JZ, Keenlyside RA, Ziegler DW, Retailliau HF, Eddins DL, Bryan JA.** 1979. Guillain-Barre syndrome following vaccination in the National Influenza Immunization Program, United States, 1976-1977. Am. J. Epidemiol. **110:**105–123.
30. **Safranek TJ, Lawrence DN, Kurland LT, Culver DH, Wiederholt WC, Hayner NS, Osterholm MT, O'Brien P, Hughes JM.** 1991. Reassessment of the association between Guillain-Barré syndrome and receipt of swine influenza vaccine in 1976-1977: results of a two-state study. Expert Neurology Group. Am. J. Epidemiol. **133:**940–951.
31. **Jonville-Béra AP, Autret E, Galy-Eyraud C, Hessel L.** 1996. Thrombocytopenic purpura after measles, mumps and rubella vaccination: a retrospective survey by the French Regional Pharmacovigilance Centres and Pasteur-Mérieux Sérums et Vaccins. Pediatr. Infect. Dis. J. **15:**44–48. http://dx.doi.org/10.1097/00006454-199601000-00010.
32. **Beeler J, Varricchio F, Wise R.** 1996. Thrombocytopenia after immunization with measles vaccines: review of the vaccine adverse events reporting system (1990 to 1994). Pediatr. Infect. Dis. J. **15:**88–90. http://dx.doi.org/10.1097/00006454-199601000-00020.
33. **Massell BF, Honikman LH, Amezcua J.** 1969. Rheumatic fever following streptococcal vaccination. Report of three cases. JAMA **207:**1115–1119.
34. **McNeil SA, Halperin SA, Langley JM, Smith B, Warren A, Sharratt GP, Baxendale DM, Reddish MA, Hu MC, Stroop SD, Linden J, Fries LF, Vink PE, Dale JB.** 2005. Safety and immunogenicity of 26-valent group A streptococcus vaccine in healthy adult volunteers. Clin. Infect. Dis. **41:**1114–1122. http://dx.doi.org/10.1086/444458.
35. **WHO.** 2005. Group A streptococcal vaccine development: current status and issues of relevance to less developed countries. WHO, Geneva, Switzerland.
36. **Martin S, Adermann K, Forssmann WG, Kuhn M.** 1999. Regulated, side-directed secretion of proguanylin from isolated rat colonic mucosa. Endocrinology **140:**5022–5029. http://dx.doi.org/10.1210/endo.140.11.7103.
37. **Garrett BM, Visweswariah SS.** 1996. A conformational epitope in the N-terminus of the Escherichia coli heat-stable enterotoxins is involved in receptor-ligand interactions. Biochim. Biophys. Acta **1317:**149–154. http://dx.doi.org/10.1016/S0925-4439(96)00047-6.
38. **Eswar N, Webb B, Marti-Renom MA, Madhusudhan MS, Eramian D, Shen M, Pieper U, Sali A.** 2006. Comparative protein structure modeling using Modeller. Curr. Protoc. Bioinformatics Chapter 5:Unit 5.6. http://dx.doi.org/10.1002/0471250953.bi0506s15.
39. **Brooks BR, Brooks CL, Mackerell AD, Nilsson L, Petrella RJ, Roux B, Won Y, Archontis G, Bartels C, Boresch S, Caflisch A, Caves L, Cui Q, Dinner AR, Feig M, Fischer S, Gao J, Hodoscek M, Im W, Kuczera K, Lazaridis T, Ma J, Ovchinnikov V, Paci E, Pastor RW, Post CB, Pu JZ, Schaefer M, Tidor B, Venable RM, Woodcock HL, Wu X, Yang W, York DM, Karplus M.** 2009. CHARMM: the biomolecular simulation program. J. Comput. Chem. **30:**1545–1614. http://dx.doi.org/10.1002/jcc.21287.
40. **Kalé L, Skeel RD, Bhandarkar M, Brunner R, Gursoy A, Krawetz N, Phillips JC, Shinozaki A, Varadarajan K, Schulten K.** 1999. NAMD2: greater scalability for parallel molecular dynamics. J. Comput. Phys. **151:**283–312. http://dx.doi.org/10.1006/jcph.1999.6201.
41. **Phillips JC, Braun R, Wang W, Gumbart J, Tajkhorshid E, Villa E, Chipot C, Skeel RD, Kalé L, Schulten K.** 2005. Scalable molecular dynamics with NAMD. J. Comput. Chem. **26:**1781–1802. http://dx.doi.org/10.1002/jcc.20289.
42. **MacKerell AD, Jr, Bashford D, Bellott M, Dunbrack RL, Jr, Evanseck JD, Field MJ, Fischer S, Gao J, Guo H, Ha S, Joseph-McCarthy D, Kuchnir L, Kuczera K, Lau FTK, Mattos C, Michnick S, Ngo T, Nguyen DT, Prodhom B, Reiher WE, Roux B, Schlenkrich M, Smith JC, Stote R, Straub J, Watanabe M, Wiórkiewicz-Kuczera J, Yin D, Karplus M.** 1998. All-atom empirical potential for molecular modeling and dynamics studies of proteins. J. Phys. Chem. B **102:**3586–3616. http://dx.doi.org/10.1021/jp973084f.
43. **Mackerell AD, Feig M, Brooks CL.** 2004. Extending the treatment of backbone energetics in protein force fields: limitations of gas-phase quantum mechanics in reproducing protein conformational distributions in molecular dynamics simulations. J. Comput. Chem. **25:**1400–1415. http://dx.doi.org/10.1002/jcc.20065.
44. **Jo S, Kim T, Iyer VG, Im W.** 2008. CHARMM-GUI: a Web-based graphical user interface for CHARMM. J. Comput. Chem. **29:**1859–1865. http://dx.doi.org/10.1002/jcc.20945.
45. **Gobom J, Nordhoff E, Mirgorodskaya E, Ekman R, Roepstorff P.** 1999. Sample purification and preparation technique based on nano-scale reversed-phase columns for the sensitive analysis of complex peptide mixtures by matrix-assisted laser desorption/ionization mass spectrometry. J. Mass Spectrom. **34:**105–116.
46. **Shevchenko A, Wilm M, Vorm O, Mann M.** 1996. Mass spectrometric sequencing of proteins silver-stained polyacrylamide gels. Anal. Chem. **68:**850–858. http://dx.doi.org/10.1021/ac950914h.
47. **Zhang W, Robertson DC, Zhang C, Bai W, Zhao M, Francis DH.** 2008. Escherichia coli constructs expressing human or porcine enterotoxins induce identical diarrheal diseases in a piglet infection model. Appl. Environ. Microbiol. **74:**5832–5837. http://dx.doi.org/10.1128/AEM.00893-08.
48. **Lauber T, Neudecker P, Rösch P, Marx UC.** 2003. Solution structure of human proguanylin: the role of a hormone prosequence. J. Biol. Chem. **278:**24118–24124. http://dx.doi.org/10.1074/jbc.M300370200.
49. **Ragvin A, Valvatne H, Erdal S, Arskog V, Tufteland KR, Breen K, Øyan AM, Eberharter A, Gibson TJ, Becker PB, Aasland R.** 2004. Nucleosome binding by the bromodomain and PHD finger of the transcriptional cofactor p300. J. Mol. Biol. **337:**773–788. http://dx.doi.org/10.1016/j.jmb.2004.01.051.
50. **Ausubel FM, Brent R, Kingston RE, Moore DD, Seidman JG, Smith JA, Struhl K, Wiley CJ, Allison RD, Bittner M, Blackshaw S (ed).** 2003. Current protocols in molecular biology. John Wiley & Sons, Inc, New York, NY.
51. **Ritz C, Streibig JC.** 2005. Bioassay analysis using R. J. Stat. Softw. **12**(5):1–22. http://www.jstatsoft.org/v12/i05/paper.